

Infinite Dilution Partial Molar Volumes of Butanal and 2-Methylpropanal in Supercritical Carbon Dioxide

Yang Guo and Aydin Akgerman*

Chemical Engineering Department, Texas A&M University, College Station, Texas 77843-3122

The partial molar volume is a very important thermodynamic property for describing the temperature and pressure effects in the supercritical fluids. We have utilized the dynamic tracer response technique to measure the infinite dilution partial molar volumes of butanal (*n*-butyraldehyde) and 2-methylpropanal (isobutyraldehyde) in supercritical carbon dioxide at 318 K and 360 K and in the pressure range of 90.6–207.8 bar.

Introduction

The research on the use of supercritical fluids (SCFs) as a medium for separation and chemical reaction has been receiving increasing attention. A unique and advantageous characteristic of SCF solvents is that the solvent properties are strong functions of pressure and/or temperature in the near critical region. Recently, Kaupp (1994) and Savage et al. (1995) reviewed the published studies on reactions in SCFs. They noted that the rate constant is a strong function of pressure and that pressure can influence selectivity for at least some reactions. We have studied propylene hydroformylation in supercritical carbon dioxide (SC CO₂) and observed that the selectivity of products, butanal (*n*-butyraldehyde) to 2-methylpropanal (isobutyraldehyde) ratio, increased with pressure at constant temperature (Guo and Akgerman, 1997). To understand the pressure effect on the reaction rate and selectivity, transition-state theory (Evans and Polanyi, 1935) is usually employed to describe the thermodynamics of solvent effect on rate constants. According to the transition-state theory, the pressure derivative of the rate constant is related to the difference between the partial molar volumes of the activated complex and the reactants

$$-R_g T \left(\frac{\partial \ln k}{\partial P} \right)_T = \bar{v}_M - \bar{v}_A - \bar{v}_B \quad (1)$$

where \bar{v} is the molar volume and the subscript M refers to the active complex and A and B refer to the reactants, k is the reaction rate constant, R_g is the gas constant, and T and P are temperature and pressure, respectively. Thus, the partial molar volume becomes a very important property for studying the pressure effect in SCFs.

The partial molar volume of the solute in the SCFs is also the key property for probing molecular interactions because of its differential nature (Brennecke and Eckert, 1989). At the vicinity of the critical point, very large negative partial molar volumes are observed (Erkey and Akgerman, 1990). This phenomenon is explained both in terms of local density enhancement called "clustering", which is due to the condensation of solvent molecules around the solute molecule, and in terms of the divergence of density fluctuations near the critical point. In any way,

* To whom all correspondence should be addressed. Tel. and Fax: 409-845-3375. Email: a-akgerman@tamu.edu.

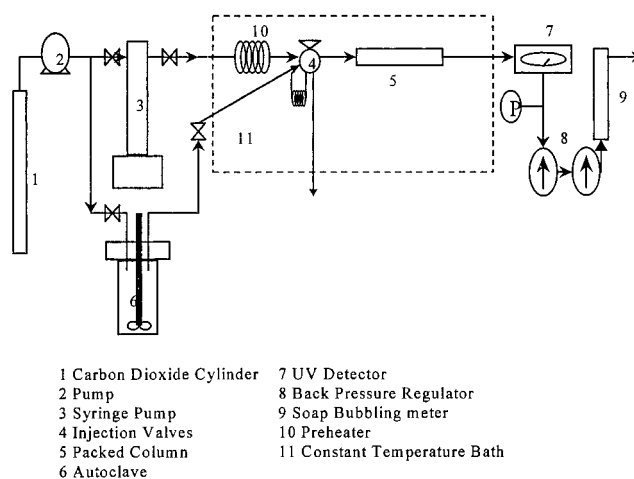


Figure 1. Schematic diagram of the experimental setup.

it is extremely important in SCF phase equilibria since it is related to the solute–solvent interactions, which in turn affect other macroscopic properties, such as solubility (Johnston et al., 1989) and reaction rates.

We have measured the adsorption equilibrium constants for butanal and 2-methylpropanal on Porapak T in the presence of SC CO₂ at 318.0 K and 360.0 K in the pressure range of 90.6–207.8 bar using the dynamic tracer response technique. The partial molar volumes of butanal and 2-methylpropanal at infinite dilution in supercritical carbon dioxide were extracted from the isothermal density dependence of the equilibrium constants.

Experimental Section

We used the dynamic tracer response technique to determine partial molar volumes in SCFs (Erkey and Akgerman, 1990). In this technique, a pulse of solute dissolved in the SC CO₂ is injected into a packed column. The solute retention time is then measured. Partial molar volumes are extracted from the density dependence of the capacity factor, which is a dimensionless retention time. A schematic diagram of the experimental setup is shown in Figure 1. Carbon dioxide (Praxair, 99.5%) was used as the carrier fluid. The syringe pump (Isco, LC-260) was filled with liquid CO₂ from the supply cylinder. The pump was started and CO₂ started to flow through the preheater,

Table 1. Properties of the Packed Bed

bed length, L	1.0 m
bed diameter	0.001 75 m
bed porosity, α	0.456
particle size	149–180 μm
particle porosity, β	0.40
particle density, ρ_p	0.636 g/mL
mean pore diameter	66.8 \AA
BET surface area	306.0 m^2/g
pore volume	0.629 cm^3/g

the adsorption column (stainless steel tubing packed with Porapak T (Alltech) particles), and the high-pressure UV detector with an internal volume of 50 μL (Dynamax UV-D II). The response of the UV detector was recorded by the computer for analysis. The system pressure was established by a back-pressure regulator (Tescom Inc.) placed after the UV detector. A second back-pressure regulator (Grove SD91XW), set at approximately 80 bar, enabled CO_2 to go through a double expansion and reduced pulsations. The system pressure was measured with Heise pressure gauge. The flow rate was measured by a soap bubble meter placed after the second back-pressure regulator.

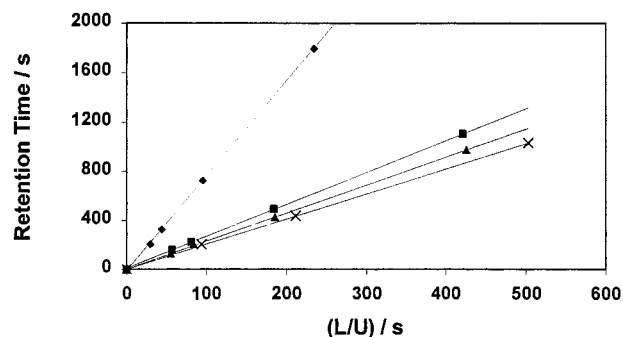
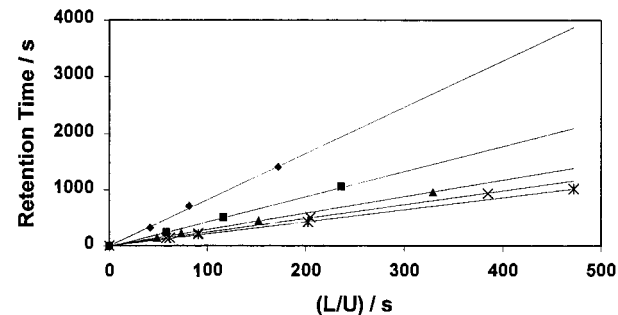
The preheater, the packed column, and the injection valve were immersed in a water bath. The temperature of the bath was controlled with an Isotemp Immersion Circulator (Fisher Scientific 730). A 20 μL pulse of butyraldehyde dissolved in CO_2 was introduced into the column through a high-pressure injection valve (Rheodyne 7010). The sample solution (1 mL of solute) was prepared in a 300 mL vessel with a Magnodrive stirrer (Autoclave Engineers). This solution was added to the sample loop (20 μL) in the injection valve. The solutes *n*-butyraldehyde (Fluka, 99%) and isobutyraldehyde (Fluka, 99%) were used as received. Porapak T (Alltech, spherical, 80/100 mesh) was used as the packing material of the column in the experiments. The particle-packed column was preheated overnight at 383 K. The bed porosity was measured by weighing a known volume of particles. The mean pore diameter, the pore volume, and the surface area of the particles were determined by nitrogen adsorption. The particle porosity was calculated on the basis of the nitrogen adsorption. The specifications of the bed and the particles are given in Table 1.

Table 2. Thermodynamic Properties of Butanal at Infinite Dilution from Supercritical Fluid Chromatography (Fluid Phase, CO_2)

T/K	P/bar	$\rho/\text{g}/\text{cm}^3$ (for CO_2)	K_T/bar^{-1} (for CO_2)	$K_A 10^3/$ (m^3/kg)	k_c	$\bar{v}^\infty/$ (cm^3/mol)
318	91.7	0.347	0.0400	8.886 ± 0.343	4.564 ± 0.176	-1242 ± 48
318	100.3	0.484	0.0329	3.861 ± 0.496	1.983 ± 0.255	-1435 ± 180
318	116.3	0.634	0.00851	1.895 ± 0.066	0.973 ± 0.034	-432.1 ± 15
318	138.8	0.714	0.00354	1.298 ± 0.150	0.667 ± 0.077	-183.4 ± 21
318	207.5	0.818	0.00125	0.873 ± 0.116	0.448 ± 0.060	-62.72 ± 8.4
360	90.8	0.178	0.0154	22.628 ± 1.41	11.623 ± 0.727	-402.2 ± 25
360	120.5	0.270	0.0130	9.271 ± 0.588	4.762 ± 0.302	-518.9 ± 33
360	144.4	0.358	0.0108	4.755 ± 0.324	2.442 ± 0.166	-469.2 ± 32
360	206.3	0.561	0.00438	1.790 ± 0.074	0.920 ± 0.038	-184.0 ± 7.6

Table 3. Thermodynamic Properties of 2-Methylpropanal at Infinite Dilution from Supercritical Fluid Chromatography (Fluid Phase, CO_2)

T/K	P/bar	$\rho/(\text{g}/\text{cm}^3)$ (for CO_2)	K_T/bar^{-1} (for CO_2)	$K_A 10^3/$ (m^3/kg)	k_c	$\bar{v}^\infty/$ (cm^3/mol)
318	91.5	0.343	0.0397	8.130 ± 0.580	4.176 ± 0.298	-1343 ± 96
318	118.6	0.646	0.00745	1.526 ± 0.185	0.784 ± 0.095	-380.1 ± 46
318	142.4	0.723	0.00321	1.087 ± 0.105	0.558 ± 0.054	-160.5 ± 15
318	206.1	0.817	0.00126	0.771 ± 0.092	0.396 ± 0.047	-57.71 ± 6.8
360	92.2	0.182	0.0153	22.455 ± 1.318	11.534 ± 0.677	-317.0 ± 19
360	121.3	0.272	0.0129	10.629 ± 0.593	5.459 ± 0.305	-448.9 ± 25
360	145.1	0.360	0.0108	5.401 ± 0.145	2.774 ± 0.074	-448.6 ± 12
360	205.8	0.559	0.0043	1.974 ± 0.145	1.014 ± 0.074	-138.2 ± 10

**Figure 2.** Change in retention time of 2-methylpropanal with flow rate at different pressures at 318 K: \blacklozenge , 91.5 bar; \blacksquare , 118.6 bar; \blacktriangle , 142.4 bar; \times , 206.1 bar.**Figure 3.** Change in retention time of butanal with flow rate at different pressures at 318 K: \blacklozenge , 91.7 bar; \blacksquare , 100.3 bar; \blacktriangle , 116.3 bar; \times , 138.8 bar; $*$, 207.5 bar.

Results and Discussion

In the experiment, a pulse of solute dissolved in the SCCO_2 was injected into the packed column. The solute retention time is given as

$$t_R = \frac{L}{U}(1 + \delta_0) \quad (2)$$

where L is the length of the column, U is the interstitial velocity, and

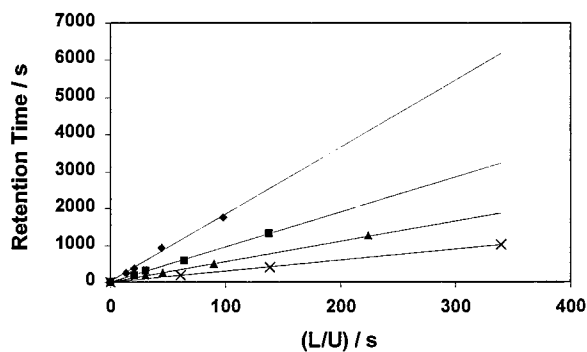


Figure 4. Change in retention time of 2-methylpropanal with flow rate at different pressures at 360 K: \blacklozenge , 92.2 bar; \blacksquare , 121.3 bar; \blacktriangle , 145.1 bar; \times , 205.8 bar.

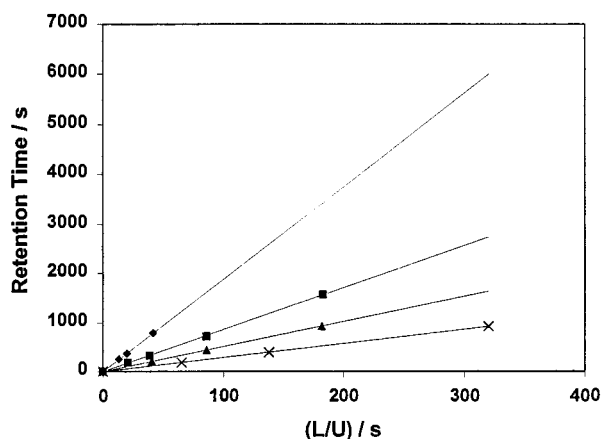


Figure 5. Change in retention time of butanal with flow rate at different pressures at 360 K: \blacklozenge , 90.8 bar; \blacksquare , 120.5 bar; \blacktriangle , 144.4 bar; \times , 206.3 bar.

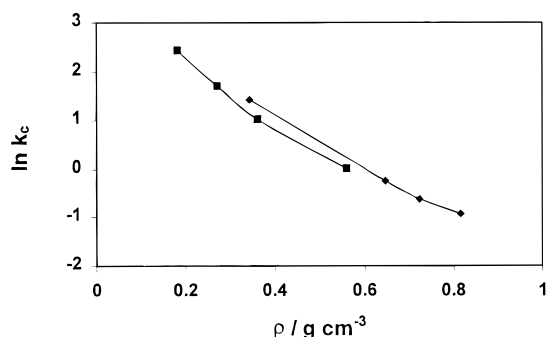


Figure 6. Variation of capacity factor with density for 2-methylpropane: \blacklozenge , 316 K; \blacksquare , 360 K.

$$\delta_0 = \frac{1 - \alpha}{\alpha} (\beta + \rho_P K_A) \quad (3)$$

where β is the particle porosity, α is the bed porosity, ρ_P is the particle density, and K_A is adsorption equilibrium constant (Wakao and Kaguei, 1982). The retention time is determined experimentally as a function of flow rate, and K_A is estimated from eqs 2 and 3 and the slope of t_R vs L/U . The data are presented in Figures 2–5 for the two compounds at the two temperatures investigated in this study. The corresponding K_A values are presented in Tables 2 and 3. A decrease in K_A values was observed with increase in density at constant temperature.

In chromatography theory, solute retention is expressed as a dimensionless residence time called the capacity factor, k_c , and the adsorption equilibrium constant is related to the capacity factor by the expression

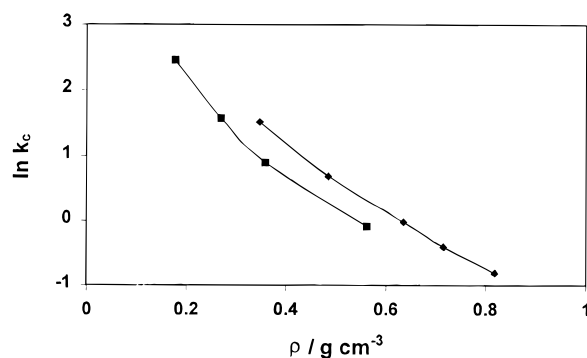


Figure 7. Variation of capacity factor with density for butanal: \blacklozenge , 318 K; \blacksquare , 360 K.

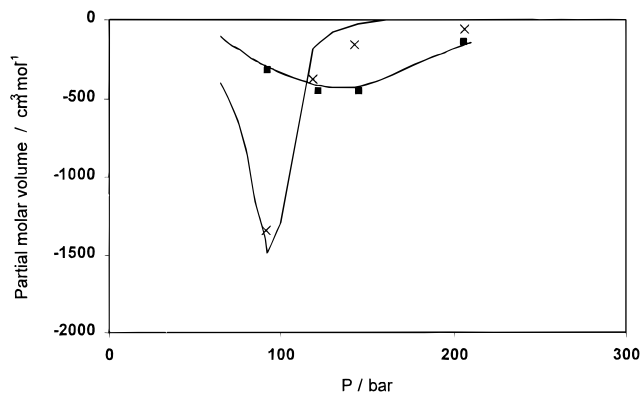


Figure 8. Partial molar volumes of isobutyraldehyde at infinite dilution in SCCO_2 as a function of pressure: \times , 318 K; \blacksquare , 360 K; —, Peng–Robinson equation fit.

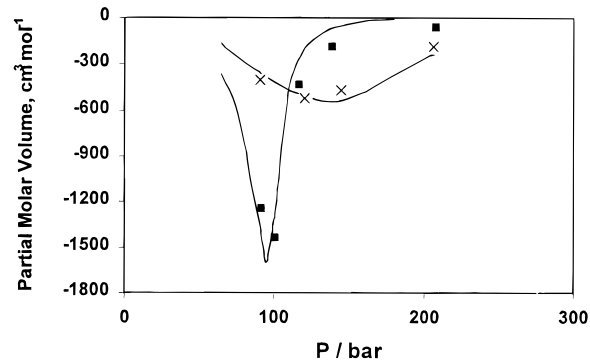


Figure 9. Partial molar volumes of *n*-butyraldehyde at infinite dilution in SCCO_2 as a function of pressure: \blacksquare , 318 K; \times , 360 K; —, Peng–Robinson equation fit.

$$k_c = \frac{(1 - \alpha)\rho_P K_A}{(1 - \alpha)\beta + \alpha} \quad (4)$$

k_c values are also listed in Tables 2 and 3. The capacity factors, on the other hand, are directly related to the partial molar volumes at infinite dilution (Chimowitz and Kelly, 1989; Shim and Johnston, 1991)

$$\rho \left(\frac{\partial \ln k_c}{\partial \rho} \right)_T = - \left(1 - \frac{\bar{v}}{R_g T K_T} \right) \quad (5)$$

where ρ is the density and K_T is the isothermal compressibility of the SCCO_2 . The density ρ and the isothermal compressibility K_T were calculated from an equation of state given by IUPAC (Angus et al., 1976). Figures 6 and 7 show the variation of the logarithm of the capacity factor with density for the two isomers at two temperatures. The

Table 4. Binary Interaction Parameters with CO₂

<i>T</i> /K	compound	<i>k_{ij}</i>
318	butanal	0.11
360	butanal	-0.15
318	2-methylpropanal	0.10
360	2-methylpropanal	-0.06

curves were fitted with a second-order polynomial, and the partial molar volumes were calculated using eq 5. Figures 8 and 9 present the infinite dilution partial molar volumes in SCCO₂ as a function of pressure at two different temperatures. The lines are the best fit using the Peng–Robinson equation of state along with van der Waals mixing rule. The binary interaction parameters regressed are listed in Table 4. It is believed that the difference between the partial molar volumes of the two isomers is what determines the change in selectivity of the reaction with pressure at constant temperature.

Literature Cited

- Angus, B.; Armstrong, A. B.; de Reuck, K. M., Eds.; *IUPAC: International Thermodynamic Tables of the Fluid State Carbon Dioxide*; Pergamon Press: New York, 1976.
- Brennecke, J. F.; Eckert, C. A. Phase Equilibria for Supercritical Fluid Process Design. *AIChE J.* **1989**, *35*, 1490.
- Chimowitz, E. H.; Kelly, F. D. A New Representation for Retention Time in Supercritical Fluid Chromatography. *J. Supercrit. Fluids* **1989**, *2*, 106.
- Erkey, C.; Akgerman, A. Chromatography Theory: Application to Supercritical Extraction. *AIChE J.* **1990**, *36*, 1715.
- Evans, M. G.; Polanyi, M. Some Applications of the Transition State Methods to the Calculation of Reaction Velocities, Especially in Solution. *Trans. Faraday Soc.* **1935**, *31*, 875.
- Guo, Y.; Akgerman, A. Hydroformylation of Propylene in Supercritical Carbon Dioxide. *Ind. Eng. Chem. Res.* **1997**, *36*, 4581.
- Johnston, K. P.; Kim, S.; Combes, J. Spectroscopic Determination of Solvent Strength and Structure in Supercritical Fluid Mixtures: A Review. In *Supercritical Fluid Science and Technology*; Johnston, K. P., Penninger, J. M. L., Eds.; American Chemical Society: Washington, DC, 1989.
- Kaupp, G. Reactions in Supercritical Carbon Dioxide. *Angew. Chem., Int. Ed. Engl.* **1994**, *33* (14), 1452.
- Savage, P. E.; Gopalan, S.; Mizan, T. I.; Martino, C. J.; Brock, E. E. Reaction at Supercritical Conditions: Applications and Fundamentals. *AIChE J.* **1995**, *41* (7), 1723.
- Shim, J.-J.; Johnston, K. P. Phase Equilibria, Partial Molar Enthalpies, and Partial Molar Volumes Determined by Supercritical Fluid Chromatography. *J. Phys. Chem.* **1991**, *95*, 353.
- Wakao, N.; Kaguei, S. *Heat and Mass Transfer in Packed Bed*; Gordon and Breach Science Publishers: New York, 1982.

Received for review March 18, 1998. Accepted June 29, 1998. This project has been funded by Grants 104TAM0441, 026TAM2441, and 027TAM3441 in part with Federal Funds as part of the program of the Gulf Coast Hazardous Substance Research Center, which is supported under cooperative agreement R815197 with the United States Environmental Protection Agency and in part with funds from the State of Texas as part of the program of the Texas Hazardous Waste Research Center. The contents do not necessarily reflect the views and policies of the U.S. EPA or the State of Texas nor does the mention of trade names or commercial product constitute endorsement or recommendation for use.

JE9800712